Comprehensively Efficient Analysis of Nonlinear Wire Scatterers Considering Lossy Ground and Multi-tone Excitations

Amir Bahrami and Saeed Reza Ostadzadeh

Department of Electrical Engineering,
Arak University, Arak, Iran
bahrami94amir@gmail.com, s-ostadzadeh@araku.ac.ir.

Abstract **─** In this paper based on intelligent water drops algorithm (IWD), comprehensively nonlinear analysis of nonlinearly loaded wire scatterers are carried out. The analyses involve two stages. First, the problem is modeled as a nonlinear multi-port equivalent circuit and it is then reformulated into an optimization problem which is solved by the IWD. The simulation results are compared with harmonic balance (HB), arithmetic operator method (AOM), approximate methods and experiment. Analysis of the problem under strongly nonlinear loads, presence of lossy ground, multi-port structures, and multi-ton excitations are included to cover all the complex aspects. In one hand, the proposed modeling approach is in excellent agreement with other conventional techniques. On the other hand, the run time is considerably reduced.

Index Terms **─** IWD, lossy ground, multi-tone excitation, nonlinear load, wire scatterers.

I. INTRODUCTION

As known, nonlinearly loaded wire scatterers in single and multi-port structures can be used in applications such as control of scattering response, microwave imaging and protecting against high-valued signals such as lightning return strokes [1-10].

In this paper, nonlinearly loaded wire scatterers as single-port and multi-port are investigated as shown in Fig. 1. Such structures are used to control scattering response at frequency harmonic of interest using tuning the spacing among antennas and respective nonlinear load. From now on, the mentioned scatterers are called nonlinear wire scatterer for simplicity. The analyses of such structures are carried out in the frequency domain [1-5], time domain [6, 7], and mixed time-frequency domain [8-10]. Although the frequency-domain methods are suitable for inclusion of frequency dependence of the lossy ground, they are limited to weakly nonlinear loads [1-3] and suffering from drawbacks of Newton Raphson algorithm [4, 5] which yields unacceptable results [5]. Time domain methods, on the other hand, are easily used to treat nonlinearity effect of arbitrary order, however, inclusion of frequency dependence effect of the lossy ground is difficult. To include both effects, the mixed time-frequency domain methods such as harmonic balance technique (HB) should be used [8-10]. In the last method, all the mentioned scatterers depending upon the number of ports are modelled as a nonlinear equivalent circuit as shown in Fig. 2. In this figure, the nonlinear circuits consists of two parts. The first part is the linear part representing Norton circuit viewed across the nonlinear load. This part includes I_{sc} as the short circuit current which is due to the applied excitation, Y_{in} and $\overline{\overline{Y}}$ as the input admittance matrix viewed across the nonlinear load at mixing frequencies respectively for single-port and multi-port scatterers. The three mentioned quantities are conventionally computed using numerical methods such as method of moments (MoM). The second part in Fig. 2 is a nonlinear part which is used for modelling the nonlinearity effects of the device connected to the wire scatterer.

The HB technique is suitable for strongly nonlinear loads, but it is inefficient in analyzing multi-port wire scatterers under multi-tone excitations. Also, it suffers from initial guess and gradient operation in the Newton Rophson iteration algorithm. To remove these drawbacks, a number of optimization techniques [11-13] such as genetic algorithm (GA) [11], and particle swarm optimization (PSO) [12]] for analysis of nonlinear wire scatterers under single tone excitation were proposed. Such approaches, although yield near global solutions, they are time-consuming especially for multi-port structures under multi-tone exciations. In addition, the mentioned Norton circuits are computed via MoM which is time consuming. To remove this complexity, Ostadzadeh et al. proposed a model based on fuzzy inference (MoF) to compute Norton circuit very efficiently [14-16]. The rest challenge is that to compute the induced voltage across the nonlinear load efficiently.

Submitted On: March 23, 2020
Accepted On: May 4, 2020
https://doi.org/10.47037/2020.ACES.J.350805

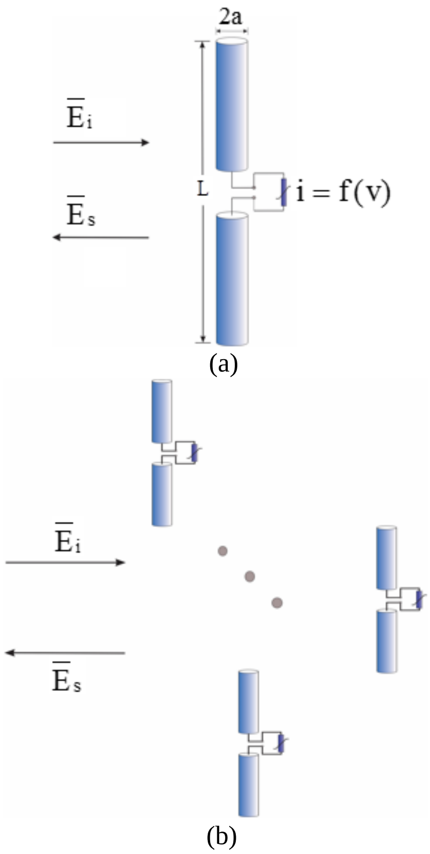

Fig. 1. Nonlinearly loaded wire scatterer as: (a) single port and (b) multi-port structures.

In our previously published literature [17], the IWD algorithm has been used for computing scattering response from Gun diode-loaded antenna array under single-tone excitation but its efficiency in the presence of lossy ground, strongly nonlinear loads and multi-tone excitations was not addressed. In this study, comprehensive analysis of nonlinear wire scatterers based on IWD algorithm considering the mentioned aspects is carried out. The simulation results show that the IWD-based results are in excellent agreement with the HB, AOM, experiment and approximate methods while the run-time is considerably reduced.

This paper is organized as follows. Section II is focused on formulation principles of the nonlinear wire scatterers. IWD algorithm is briefly explained in Section III. Section IV applies the IWD on the multi-port nonlinear wire scatterers considering different complex aspects. Finally conclusion is given in Section V.

II. ANALYSIS OF NONLINEAR WIRE SCATTERERS

As known, the main problem in analyzing nonlinear wire scatterers is compution of the induced voltage across the nonlinear load. To this end, the following cost function should be zero [8]:

$$\left|\bar{\varepsilon}\right| = \left|\bar{\bar{Y}}_{in}\bar{V}_s - \bar{I}_{sc} + \bar{\bar{D}}f\left(\bar{\bar{T}}\bar{V}_s\right)\right| \to \bar{0}. \qquad (1)$$

All quantities in (1) are defined as below:

$\bar{I}_{sc}$ is a vector of short-circuit currents due to the excitations which is computed only at M excitation frequencies, that is,

$$\bar{I}_{sc} = [I_0 \quad I_{1r} \quad I_{1i} \quad \cdots \quad I_{Mr} \quad I_{Mi}]. \qquad (2)$$

$\bar{\bar{Y}}_{in}$ is a matrix containing input admittance viewed across the nonlinear load at N mixing frequencies (N>M), that is,

$$\bar{\bar{Y}}_{in} = \begin{bmatrix} 0 & 0 & 0 & \dots & 0 & 0 \\ 0 & G_{in1} & B_{in1} & 0 & \vdots & 0 \\ 0 & -B_{in1} & G_{in1} & \ddots & 0 & \vdots \\ \vdots & 0 & 0 & \ddots & & 0 \\ 0 & \vdots & \vdots & 0 & G_{inN} & B_{inN} \\ 0 & 0 & \cdots & 0 & -B_{inN} & G_{inN} \end{bmatrix}. \qquad (3)$$

$\bar{\bar{D}}$ and $\bar{\bar{T}}$ are respectively transformation matrix from the frequency domain to the time domain and vice versa. Also, $f(.)$ is the (i-v) characteristic of the nonlinear load. All the above quantities are known, except $\bar{V}_s$, which is an unknown vector including induced voltages across nonlinear load at N mixing harmonic frequencies as follows:

$$\bar{V}_{sc} = [V_0 \quad V_{1r} \quad V_{1i} \quad \cdots \quad V_{Nr} \quad V_{Ni}]. \qquad (4)$$

The vectors of $\bar{V}_s$ and $\bar{I}_{sc}$ are Fourier coefficients of the time-domain signals $i_{sc}(t)$ and $v(t)$, i.e.,

$$i_{sc}(t) = I_0 + \sum_{j=1}^{M}\{I_{jr}\cos(\omega_j t) + I_{ji}\sin(\omega_j t)\}, \qquad (5)$$

$$v(t) = V_0 + \sum_{j=1}^{N}\{V_{jr}\cos(\omega_j t) + V_{ji}\sin(\omega_j t)\}. \qquad (6)$$

In dealing with Multi-port nonlinear wire scatterers, the input admittance matrix $\bar{\bar{Y}}_{in}$ is replaced with the admittance matrix $\bar{\bar{Y}}$ as (7) in which diagonal elements are self-admittances which are approximately the one in single-port nonlinear wire scatterers, whereas off-diagonal ones are mutual admittances between among scatterers.

To solve Eq. (1) with guaranteed convergence, we resort to the intelligent water drop algorithm (IWD):

$$\bar{\bar{Y}} = \begin{bmatrix} Y_{11} & \cdots & Y_{1M} \\ \vdots & \ddots & \vdots \\ Y_{M1} & \cdots & Y_{MM} \end{bmatrix}. \qquad (7)$$

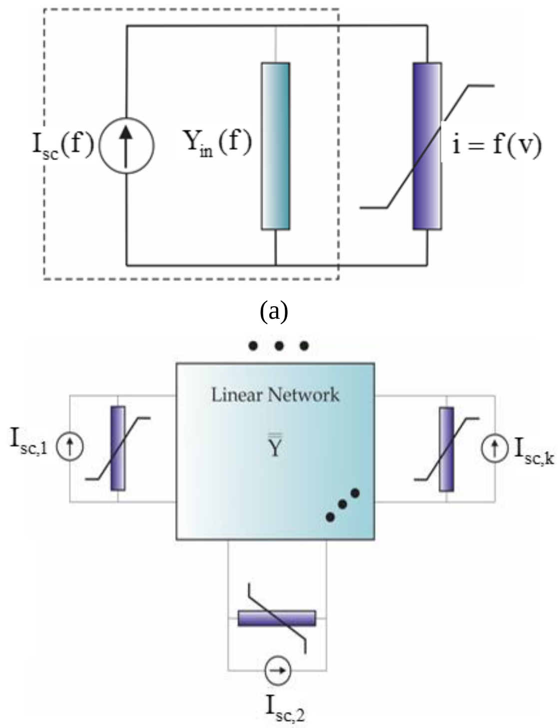

(b)

Fig. 2. Equivalent circuit of nonlinear wire scatterer as: (a) single-port and (b) multi-port structures.

III. IWD-BASED ALGORITHM

In this section, a succinct but nevertheless comprehensive explanation of the IWD algorithm is provided. The IWD algorithm is a constructive-based method, where a set of water drops move from one node to the next until a complete population of the solution is reached. This algorithm is based on the observation of the flow of water in rivers. The water in rivers is seen as a collection of water drops that flow from point in high terrain (source) to point in low terrain (destination) with a certain velocity. The water drops also carry some amount of soil with them while flowing along a path. Therefore, water drops are able to transport an amount of soil from one place to another. The parameters involved in this algorithm are classified into two kinds of static and dynamic parameters. Static parameters should be initialized before the algorithm starts, while dynamic parameters, as their name suggests, will vary as the algorithm iterates. By taking these two properties of water drops into account, IWD algorithm has been developed.

In summary, the algorithm of IWD as step by step is as follows:

1. Initialize the static parameters. The graph (V, E) of the problem is given to the algorithm. The value of the total-best solution T^{TBest}, is initially assigned to the worst value:

$$q(T^{TBest}) = -\infty . \tag{8}$$

The value of it_{max} is specified by the user. The initial value of the iteration counter is set to zero. That is $it_{count}=0$. The algorithm terminates when $it_{count}=it_{max}$.

The value of N_{IWD} (number of water drops) is set to a positive integer value, which is normally set to the number of nodes N_C in the graph. The location vector of each water drop represents the induced voltage at scatterer terminal in our problem. For soil updating a_s, b_s and c_s for velocity updating, the parameters are a_v, b_v and c_v. The local soil updating parameter ρ_n, which is a small positive number less than one, is set as $\rho_n = 0.99$. The global soil updating parameter ρ^{IWD}, which is selected from [0, 1], is set as $\rho^{IWD} = 0.99$. Furthermore, the initial soil on each path (edge) is denoted by the constant InitialSoil such as the soil of the path within every two nodes i and j, that is set by soil(i,j)=InitialSoil. The initial velocity value of each IWD is set to InitialVel. Both parameters InitialSoil and InitialVel are users choose and they should be tuned experimentally for the application.

2. Initialize the dynamic parameters. Every IWD has a visited node list V_c(IWD), which is initially empty: $V_c(IWD)=\{ \}$; Each IWD's velocity is set to InitialVel.
3. Spread the intelligent water drops randomly on the nodes of the graph as their first visited nodes.
4. Update the visited node list for each intelligent water drop to include the nodes that just visited.
5. Repeat steps 5.1 to 5.4 for those IWDs with partial solutions. Worth mentioning that partial solutions are solutions with certain degree of undesirability. Although partial solutions are not local solutions and are merely acceptable, they are not the optimum solution.

5.1) Consider water drop k residing at the current node (node i) intends to move to the next node (node j) through an edge e(i,j). The edge selection is done through a probability function, determined by $P_i^{IWD}(j)$, as defined in (2). Then, the water drop visits node j by adding to V_c(IWD):

$$P_i^{IWD}(j) = \frac{d(soil(i,j))}{\sum_{k \notin V_c(IWD)} soil(i,k)} , \tag{9}$$

$$d(i,j) = \frac{1}{\varepsilon + g(soil(i,j))} , \tag{10}$$

where ε is a small positive number used to prevent the division by zero in function d(.), and,

$$g(soil(i,j)) = \begin{cases} soil(i,j) & \text{if} \quad \min_{l \notin V_c(IWD)}(soil(i,j)) \geq 0 \\ soil(i,j) - \min_{l \notin V_c(IWD)}(soil(i,h)) & \text{else} \end{cases} , \tag{11}$$

where soil(i, j) refers to the amount of soil within the local path between nodes i and j. Then, add the newly visited node j to the list V_c(IWD).

5.2) For each IWD moving from node i to node j, update its velocity $velocity^{IWD}(t)$ by:

$$velocity^{IWD}(t+1) = velocity^{IWD}(t) + \frac{a_v}{b_v + c_v soil^2(i,j)}, \quad (12)$$

where a_v, b_v and c_v are the static parameters used to represent the nonlinear relationship between the velocity of water drop, i.e. $velocity^{IWD}$, and $velocity^{IWD}(t+1)$ is the updated velocity for the IWD.

5.3) For the intelligent water drop (IWD) moving on the path from node i to j, compute the change of soil $\Delta Soil(i, j)$ that the intelligent water drop (IWD) loads from the path by:

$$\Delta soil(i,j) = \frac{a_s}{b_s + c_s time(i,j;Vel^{IWD})}, \quad (13)$$

where, a_s, b_s, and c_s are the static parameters used to represent the nonlinear relationship between $\Delta Soil(i, j)$ and the inverse of vel^{IWD}.

Note that $time(i,j;vel^{IWD})$ refers to the time needed for water drop to transit from node i to node j at time t + 1. It is defined as follows:

$$time(i,j;Vel^{IWD}) = \frac{HUD}{\max(\varepsilon, Vel^{IWD})}, \quad (14)$$

where $HUD(.)$ is a local heuristic function defined to measure the degree of the undesirability of IWD to move between nodes i and j. In our application, it is chosen to be unity.

5.4) Update the soil Soil(i, j) of the path from node i to j traversed by that IWD and also update the soil that the IWD carries $Soil^{IWD}$ by:

$$soil(i,j) = (1-\rho).soil(i,j) - \rho.soil(i,j), \quad (15)$$

$$soil^{IWD} = soil^{IWD} - \Delta soil(i,j), \quad (16)$$

where ρ is a small positive constant between zero and one.

6) Find the iteration best solution T^{TBest} from all the solutions T^{IWD} found by the IWDs using:

$$T^{TBest} = \arg\max_{\forall T^{IWD}} q(T^{IWD}). \quad (17)$$

7) Update the soils on the paths that form the current iteration best solution T^{TBest} by:

$$soil(i,j) = (1-\rho)soil(i,j) + \rho \frac{2soil^{IWD}}{N_c(N_c - 1)}$$

$$\forall (i,j) \in T_M. \quad (18)$$

Update the total best solution T^{TBest} by the current iteration best solution T^{TBest} using:

$$T^{TBest} = \begin{cases} T^{1Best} & \text{if} \quad q(T^{TBest}) \geq q(T^{1Best}) \\ T^{TBest} & \text{else} \end{cases}. \quad (19)$$

8) Increment the iteration value by:

$$It_{count} = It_{count} + 1, \quad (22)$$

Then, go to Step 2 if:

$$It_{count} < It_{max}. \quad (21)$$

9) The algorithm stops here with the total best solution T^{1Best}.

Here T^{TBest} is the best value for harmonics voltages. It_{count} is the number of iterations when the algorithm has converged. The static and dynamic parameters in this paper are listed in Table 1 in [17].

IV. NUMERICAL SIMULATION AND DISCUSSION

A. Comparison with AOM

A.1. Strongly nonlinear load

To show the capability of the algorithm on the order of load nonlinearity, a single-port wire scatterer having length to diameter ratio L/2a=74.2, and one meter length (L=1 m) is selected. Also, the scatterer is illuminated by an incident plane wave of magnitude $E_i = 1(V/m)$ and centrally loaded with a very strongly nonlinear device, which is characterized by (22):

$$i = 10^{11} \times v^{13}. \quad (22)$$

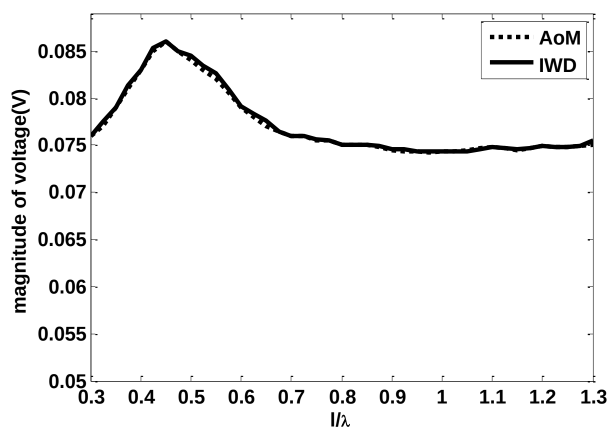

Fig. 3. The induced voltage across the strongly nonlinear load at the fundamental harmony under single-tone excitation.

Prior to analysis, the Norton circuit in Fig. 2 is efficiently computed based on [14, 15]. The voltage magnitudes for various values of length to wavelength are shown in Fig. 3. A comparison of IWD results with those obtained by the AOM [4] substantiates the high accuracy of the algorithm while the run-time is considerably reduced which will be discussed in next sections.

A.2. Lossy ground

In the second example, the versatility of the method considering lossy ground is tested. Hence, a single–port nonlinear wire scatterer is situated 0.4 m above a lossy ground, while it is illuminated by a plane wave with the polar angle of incidence θ=60 deg. The ground is characterized by a relative permittivity of ε_r=10 and conductivity of σ=0.003S/m. The nonlinear load has a (i-v) characteristic as below:

$$i = \frac{1}{75} v + 4v^3 . \qquad (23)$$

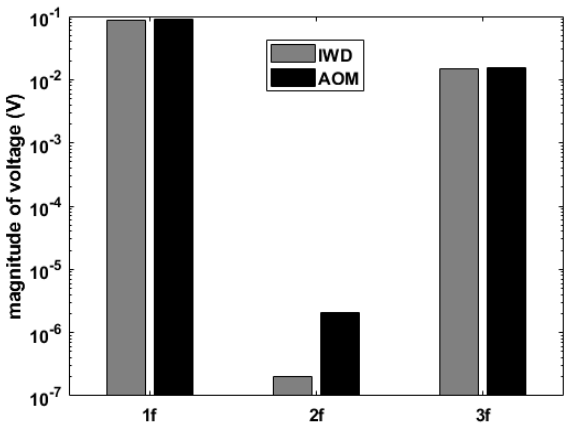

Fig. 4. Spectral content across the nonlinear load of single-port nonlinear wire scatterer over lossy ground.

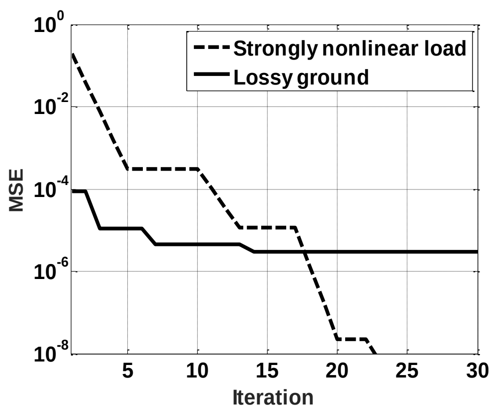

Fig. 5. Mean square error (MSE) versus iteration by the IWD approach for single nonlinear scatterer considering the lossy ground and strongly nonlinear load.

At first, the Norton circuit is efficiently computed based on the MoF in [16] and the IWD is then applied to Eq. (1). The voltage magnitudes are depicted in Fig. 5. A comparison of our results with those obtained by AOM [4] corroborates the accuracy of the proposed method. It should be mentioned that in this examples, the suppression of even harmonics are due to the cubic nature of the load's nonlinearity. As shown in Fig. 4, this even harmonic suppression is better demonstrated by the proposed method with respect to AOM. The mean square errors (MSEs) by the IWD, for the two mentioned cases are also provided in figure 5 for the first 30 iterations with deactivated stopping criteria (1.E-8). It shows that iteration process larger than 30 gives excellent agreement in the two examples.

B. Comparison with HB and NC

B.1. Single-port

In this sub-section, capability of the IWD method in comparison with HB technique [8] is investigated. Hence, a single-port wire scatterer the same as previous sections is exposed to multiple plane waves of the same amplitude (E_i =1(V/m)) and different frequencies, i.e., 140MHz, 160MHz.

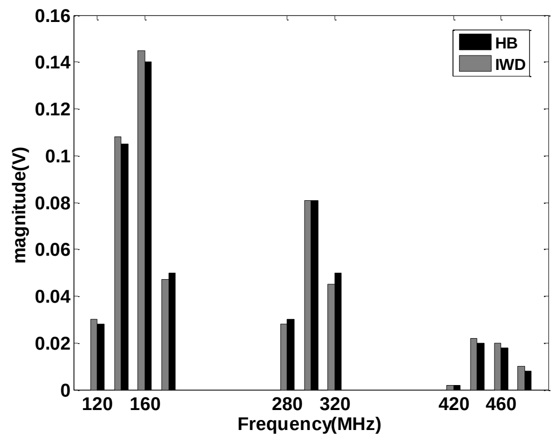

Fig. 6. Induced voltage using IWD and HB-based methods for single-port nonlinear wire scatterers.

The scatterer is centerally loaded with a p-n junction diode with the following (i-v) characteristic:

$$i = I_s (e^{v/v_T} - 1) , \qquad (24)$$

where $I_s = 10\,nA$, and $v_T = 26mV$. The induced voltage across the diode at different harmonic frequencies using the IWD, HB, and NC methods are shown in Fig. 6. From this figure, IWD and HB-based results are in good agreement, whereas the NC-based results are considerably violated.

B.1. Multi-port

In this section to show capability of the IWD in analyzing multi-port wire scatterer under multi-ton excitation, an infinite planar array of nonlinear wire scatterers is chosen. The scatterers in the array are equally spaced in vertical and horizontal directions. The nonlinear wire scatterers in the array are the same as the previous sub-sections. The induced voltage across the p-n junction diode are computed for the vertical and horizontal spacing 1 m and shown in Fig. 7.

The HB and NC-based results are included in the same figure as well. From this figure, IWD-based results are in good agreement with HB-based ones [18]. In addition, although the approximated method of NC is efficient, it is violated under strong nonlinearity.

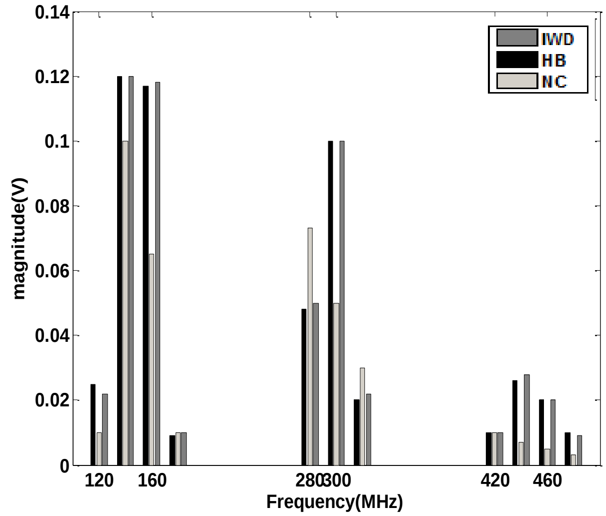

Fig. 7. The induced voltage across the diode at different harmonics for multi-port nonlinear wire scatterers.

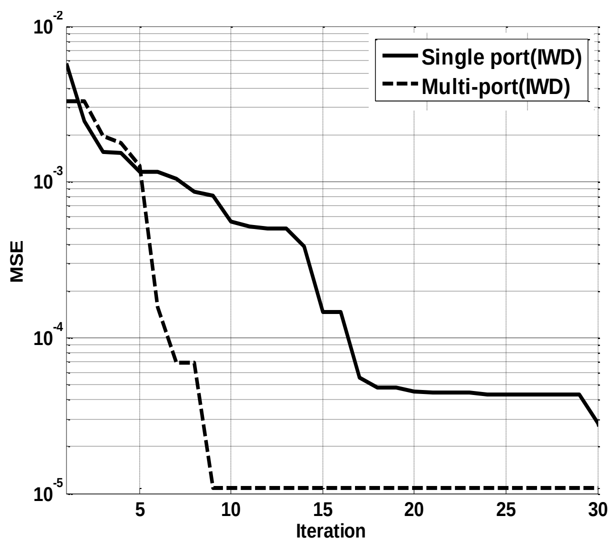

Fig. 8. The MSEs for single and multi-port nonlinear wire scatterer.

To show the efficiency of the proposed approach better, the MSEs for the single and multi-port nonlinear wire scatterers with very fast convergences are shown in Fig. 8. Finally, the relative error percentages of the proosed method for single and multi-port wire scatterers in comparision with the HB technique are listed in Table 1. From this table, the precise of the IWD can be observed.

Table 1: Relative error percentage of the IWD algorithm in comparison with the HB technique at different harmonic frequencies

Relative Error Percentage of Terminal Voltage						
f (MHz)	**120**	**140**	**160**	**180**	**280**	**300**
Single port	6.7	2.7	3.5	6	9	2.2
Multi port	7.2	0.5	2.4	3.5	8.3	0.8
f (MHz)	**320**	**420**	**440**	**460**	**480**	**Dc**
Single port	4	0.8	9	9.5	3.5	0
Multi port	3.5	0.5	8.5	3.5	2.7	0

C. Comparison with measurement

C.1. Single-port

To illustrate another capability of the proposed approach, it is compared with measurement. Figure 9 shows complex wire scatterer namely vertical rod as single-and multi-port structures which are buried in a lossy ground and subjected to the high-valued lightning stroke. In this figure, the nonlinear load represents the ionization phenomenon in the lossy ground. The (i-v) characteristic of the nonlinear load is conventionally is expressed as follows [19]:

$$v = \frac{R}{\sqrt{1 + i / I_g}} i , \qquad (25)$$

where R is low-frequency resistance of the grounding rod, and I_g is computed as below:

$$I_g = E_c / (2\pi R^2 \sigma) , \qquad (26)$$

where E_c and σ are respectively critical electric field and conductivity of the lossy ground. Transient analysis of such scatterers has been carried out in time domain [20] where the input admittance is first computed in the frequency domain and then converted to time domain by vector fitting method [21]. Consequently, such analysis demands more run-time. Also, more recently, the ionization phenomenon has been modelled as gradually increasing radius of the rod by the MTL [22-26]. This approach, however, can not include the hystersis effect in the ionization process, whereas, by the proposed model in Fig. 9, it can be easily included [27, 28].

To verify the performance of the IWD in such complex scatterers, a vertical rod with length L=3.05m, and radius a=12.7mm and buried in a lossy ground with conductivity $\sigma = 0.011 \mathrm{S/m}$, relative permittivity $\varepsilon_r = 10$ and critical electric field $E_c = 127 \mathrm{kV/m}$ is selected [29]. The lightning stroke is expressed as a current source and shown in Fig. 12 (dotted line). Prior to analysis, such current source is represented as Fourier series, and the input admittance in Fig. 2 (a) is then computed by MoM or the efficient method based on fuzzy inference (MoF) [30, 31]. Finally, applying the IWD method to Fig. 2 (a), the lightning-induced voltage in time domain is efficiently computed and shown in figure 10 which is in good agreement with measurement [29] (Fig. 6 in [29]). The slight error shown in tail time may be due to truncation error of the Fourier series which is used to obtain the lightning current.

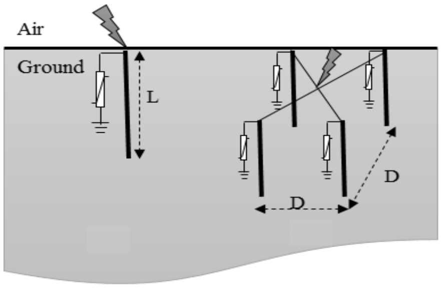

Fig. 9. Two nonlinear wire scatterers under lightning strokes as: (a): single-port rod, and (b): multi-port rod.

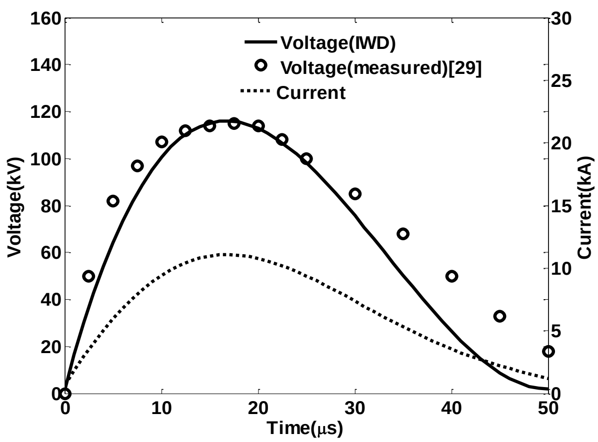

Fig. 10. Lightning-iduced voltage of the single-port vertical rod in time domain.

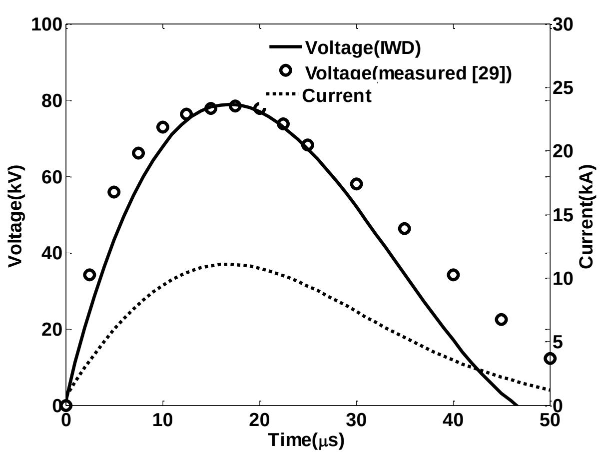

Fig. 11. Lightning-induced voltage of the multi-port vertical rod in time domain.

It's worth mentioning that the HB technique is evidently inefficient for nonlinear multi-port networks under multi-tone excitations [8]. Hence, the single-port nonlinear scatterer only has been analyzed by Shariatinasab et al. [28] and the multi-port one has not been addressed yet, whereas the proposed method can be easily applied.

C.2. Multi-port

The analysis of multi-port rod by the IWD is the same as single port, except that Fig. 2 (b) is used. Each vertical rod has length L=3.05m, and radius a=12.7mm and buried in a lossy ground with $\sigma = 0.016\mathrm{S/m}$, $\varepsilon_r = 10$ and $E_c = 50\,\mathrm{kV/m}$ [29]. The spacing between rods is D=3.09 mand the lightning current is the same as previous sub-section. The lightning-induced voltage by the IWD is shown in Fig. 11 which is in good agreement with the measurement [29] (Fig. 9 in [29]). Note that the validity of the IWD method with commercial packages has been investigated [32].

D. Comparison of run-times

As a final advantage of the IWD method, the its run-time in analyzing single and multi-port nonlinear wire scatterers under multi-tone excitations is compared with the mentioned methods.

D.1. Single-port

In the case of single-port scatterer, the wire scatterer is the one in the sub-section IV-A, and the nonlinear load is as Eq. (23). The run-times of different approaches are listed in Table 2. From this table, when the number of exciting frequencies is increased, the run-time of the IWD method is slightly increased. Moreover, although the run-time of NC-based method is very short, it is restricted to weakly nonlinear loads (Figs. 6 and 7).

D.2. Multi-port

In the case of multi-port nonlinear wire scatterers, the nonlinear load and wire scatterer are the same as previous sub-section, but the different arrangements of wire scatterers are investigated. The run-times of the different arrangements under double-ton excitation are listed in Table 3. From this table, high efficiency of the IWD in comparison with the others is once more proven.

Table 2: Run-time of different methods for single-port nonlinear wire scatterers under multi-tone excitation

Exciting Frequency (MHz)	Run-time (sec)			
	IWD	AOM	HB	NC
150	1	1	62	0.12
140,160	2	2	113	0.14
140,160,180	6	10	163	0.17
140,160,180, 200	17	31	320	0.25
140,160,180, 200,220	29	53	430	0.35

Table 3: Run-time of different methods for multi-port nonlinear wire scatterers under double-tone excitation

Multi-port Scatterer	**Run-time (sec)**			
	IWD	**AOM**	**HB**	**NC**
1 by 1	2	2	113	0.14
2 by 1	20	30	205	0.20
2 by 2	30	83	445	0.25
3 by 3	53	170	580	0.28

V. CONCLUSION

In this study, an efficient hybrid method for analyzing nonlinear wire scatterers over lossy ground under multi-ton excitations was proposed. The proposed method consists of linear and nonlinear parts. The linear part can be used for inclusion of frequency dependence of the lossy ground, while the nonlinear one considers nonlinearity effects of the device connected to the scatterer so that both effects are considered. The model was validated using extensive examples. Comparative studies show excellent agreement with the existing methods, while run-time is considerably reduced.

It worth noting that although all the nonlinear loads in this study are expressed as analytical models, the (i-v) characteristics of some of devices are based on experimental measurements and are not smooth curves [33, 34] (Fig. 7 in [33] and Table 2 in [34]). In such cases, the HB method which needs initial guess and gradient operation in the iteration process, may yield violated solutions, whereas the artificial intelligent (AI) approaches especially IWD outperforms the HB method.

REFERENCES

[1] T. K. Sarkar and D. D. Weiner, “Scattering analysis of nonlinearly loaded dipole antennas,” *IEEE Trans. Antenna Propag*., vol. 24, no. 2, pp. 125-131, 1976.

[2] T. K. Sarkar and D. D. Weiner, “Analysis of nonlinearly loaded multiport antenna structures over an imperfect ground plane using the Volterra-series method,” *IEEE Trans. Electromag. Compat.*, vol. 20, no. 2, pp. 278-287, 1978.

[3] K. C. Lee, “Mutual coupling mechanisms within arrays of nonlinear antennas,” *IEEE Trans. Electro. Compat*., vol. 47, no. 4, pp. 963-970, 2005.

[4] K. Sheshyekani, S. H. Sadeghi, and R. Moini, “A combined MoM-AOM approach for frequency domain analysis of nonlinearly loaded antennas in the presence of a lossy ground,” *IEEE Trans. Antennas Propagat*., vol. 56, no. 6, pp. 1717-1724, 2008.

[5] K. Sheshyekani, S. H. H. Sadeghi, R. Moini, and F. Rachidi, “Frequency-domain analysis of ground electrodes buried in an ionized soil when subjected to surge currents: A MoM–AOM approach,” *Electric Power System Research*, vol. 81, pp. 290-296, 2011.

[6] J. A. Landt, “Network loading of thin-wire antennas and scatterers in the time domain,” *Radio Sci*., vol. 16, pp. 1241-1247, 1981.

[7] D. Poljak, C. Y. Tham, and A. McCowen, “Transient response of nonlinearly loaded wire antennas in two-media configuration,” *IEEE Trans. Electromag. Compat.*, vol. 46, no. 1, pp. 121-125, 2004.

[8] C. C. Huang and T. H. Chu, “Analysis of wire scatterers with nonlinear or time-harmonic loads in the frequency domain,” *IEEE Trans. Antennas Propagat.*, vol. 41, no. 1, pp. 25-30, 1993.

[9] D. Liao, “Generalized wideband harmonic imaging of nonlinearly loaded scatterers,” *IEEE Trans. Antennas Propagat.*, vol. 63, no. 5, pp. 2079-2087, 2015.

[10] A. E. Yilmaz, “An envelope tracking hybrid field-circuit simulator for narrow-band analysis of nonlinearly loaded wire antennas,” *IEEE Trans. Microw. Theory and Techn.*, vol. 62, no. 2, pp. 208-223, 2014.

[11] M. Teimoori, S. R. Ostadzadeh, and B. Abdoli, “Analysis of frequency selective with nonlinear antenna under radiations of bi-frequency waves based on genetic algorithm,” *International Journal of Computer & Technology*, vol. 15, no. 7, pp. 6914-6922, 2016.

[12] K. C. Lee, “Analyses of nonlinearly loaded antennas and antenna arrays using particle swarm algorithm,” *IEEE Conference on Antennas Propag.*, 2004.

[13] S. R. Ostadzadeh, “Nonlinear analysis of non-linearly loaded dipole antenna in the frequency domain using fuzzy inference,” *Journal of Communication Engineering*, vol. 3, no. 2, pp. 141-152, 2014.

[14] S. R. Ostadzadeh, M. Tayarani, and M. Soleimani, “A fuzzy model for computing input impedance of two coupled dipole antennas in the echelon form,” *Progress in Electromagnetics Research*, vol. 78, pp. 265-283, 2008.

[15] S. R Ostadzadeh, M. Tayarani, and M. Soleimani, “A hybrid model in analyzing nonlinearly loaded dipole antenna and finite antenna array in the frequency domain,” *International Journal of RF and Microwave*, vol. 19, pp. 512-518, 2009.

[16] S. R Ostadzadeh, “An efficient hybrid model in analyzing nonlinearly loaded dipole antenna above lossy ground in the frequency domain,” *Applied Computational Electromagnetic Society (ACES) Journal*, vol. 28, no. 9, pp.780-787, 2013.

[17] A. Bahrami and S. R. Ostadzadeh, “Back scattering response from single, finite and infinite array of nonlinear antennas based on intelligent water drops algorithm,” *International Journal for Computation and Mathematics in Electrical and Electronic Engineering*, vol. 38, no. 6, pp. 2040-2056, 2019.

[18] K. C. Lee, "Two efficient algorithms for the analyses of a nonlinearly loaded antenna and antenna array in the frequency domain," *IEEE Trans. Electromag. Compat.*, vol. 45, no. 4, pp. 339-346, 2000.
[19] L. Grcev, "Modeling of grounding electrodes under lightning currents," *IEEE Trans. Electromagn. Compat.*, vol. 51, no. 3, pp. 559-571, 2009.
[20] M. Kazemi, and S. R. Ostadzadeh, "Vector fitting-based models of vertical and horizontal electrodes under lightning strikes to interface with EMTP," *Asian Journal of Fuzzy and Applied Mathematics*, vol.3, no. 1, pp. 11-21, 2015.
[21] S. Mehrabi and S. R. Ostadzadeh, "Impact of ocean-land mixed propagation path on equivalent circuit of grounding rods", *Journal of Communication Engineering*, vol. 8, no. 2, pp. 197-207, 2019.
[22] S. S. Sajjadi and S. R. Ostadzadeh, "Lightning response of multi-port grounding grids buried in dispersive soils: An approximation versus full wave methods and experiment," *Advanced Electromagnetics*, vol. 8, no. 1, pp. 43-50, 2019.
[23] S. S. Sajjadi, V. Aghajani, and S. R. Ostadzadeh, "Transient analyses of grounding electrodes considering ionization and dispersion aspects of soils simultaneously: An improved multiconductor transmission line model (Improved MTL)," *Applied Computational Electromagnetic Society Journal (ACES)*, vol. 34, no. 5, pp. 731-737, 2019.
[24] S. S. Sajjadi, V. Aghajani, and S. R. Ostadzadeh, "Comprehensive formulae for effective length of multiple grounding electrodes considering different aspects of soils: Simplified multiconductor transmission line-intelligent water drop approach," *Int. J Numer Model El.*, 2020. e2721, https://doi.org/10.1002/jnm.2721
[25] S. R. Ostadzadeh, "Validity of improved MTL for effective length of counterpoise wires under low and high-valued lightning currents," *Advanced Electromagnetics*, vol. 9, no. 1, 2020.
[26] V. Aghajani, S. S. Sajjadi, and S. R. Ostadzadeh, "Design of grounding vertical rods buried in complex soils using radial basis functions," *Journal of Communication Engineering*, vol. 7, no. 2, pp. 30-40, 2018.
[27] M. Mokhtari and G. B. Gharehpetian, "Integration of energy balance of soil ionization in CIGRE grounding electrode resistance model," *IEEE Trans. Electromagn. Compat*., vol. 60, no. 2, pp. 402-413, 2017.
[28] J. G. Safar, R. Shariatinasab, and J. He, "Comprehensive modeling of grounding electrodes buried in ionized soil based on MoM-HBM approach," *IEEE Trans. Power. Del*., vol. 57, no. 6, pp. 1627-1636, 2019.
[29] A. C. Liew and M. Darveniza, "Dynamic model of impulse characteristics of concentrated earths," *Proc. IEE*, vol. 121, no. 2, 1974.
[30] S. M. Taghavi and S. R. Ostadzadeh, "High frequency analysis of single overhead line terminated to grounding arrester using fuzzy inference models," *Journal of Communication Engineering*, vol. 2, no. 3, pp. 208-221, 2013.
[31] Z. Samiee and S. R. Ostadzadeh, "Transient analyses of grounding systems subjected by lightning surge currents through fuzzy-based models of input impedance in the frequency domain," *Asian Journal of Fuzzy and Applied Mathematics*, vol.3, no. 1, pp. 22-34, 2015.
[32] H. Samiian, S. R. Ostadzadeh, and A. Mirzaie, "Application of intelligent water drops in transient analysis of single conductor overhead lines terminated to grid-grounded arrester under direct lightning strikes," *Journal of Communication Engineering*, vol. 5, pp. 50-59, 2016.
[33] J. C. Salari and C. Portela, "Grounding systems modeling including soil ionization," *IEEE Trans. Power. Del*., vol. 23, no. 4, pp. 1939-1945, 2008.
[34] A. Geri and E. Garbagnati, "Non-linear behavior of ground electrodes under lightning surge currents: Computer modelling and comparison with experimental results," *IEEE Transactions on Magnetics*, vol. 28, no. 2, pp. 1442-1445, 1992.

Amir Bahrami was born in Esfahan, Iran, on June 22, 1994. He received B.Sc. in Electrical Engineering from Arak University, Arak, Iran, in 2016. His research interests include nonlinear microwaves, nonlinear RF circuits, nonlinear differential equations and nonlinear functional analysis.

Saeed Reza Ostadzadeh was born in Kashan, Iran, on April 13, 1978. He received B.Sc., M.Sc. and Ph.D. in Communication Engineering from the Iran University of Science and Technology (IUST), Tehran, Iran, in 2000, 2002 and 2008, respectively. He is currently an Assistant Professor in the Department of Electrical Engineering at Arak University, Arak, Iran. His research interests include qualitative modeling, grounding systems and power systems under lightning strokes. He has authored more than 50 scientific papers for conferences and international journals. He is a member of Iranian electromagnetic engineering society and Iranian fuzzy systems society.